Journal of Trace Elements in Medicine and Biology 55 (2019) 180–189

Contents lists available at ScienceDirect

Journal of Trace Elements in Medicine and Biology

journal homepage: www.elsevier.com/locate/jtemb

Pharmacology

Antitumor action of diphenyl diselenide nanocapsules: In vitro assessments and preclinical evidence in an animal model of glioblastoma multiforme

Luana Mota Ferreira[a], Juliana Hofstatter Azambuja[b], Elita Ferreira da Silveira[c], Marcel Henrique Marcondes Sari[a,d], Bruna da Cruz Weber Fulco[d], Vinicius Costa Prado[d], Nicolly Espindola Gelsleichter[b], Liziane Raquel Beckenkamp[b], Marilda da Cruz Fernandes[e], Rosélia Maria Spanevello[c], Marcia Rosângela Wink[b], Rita de Cassia Sant Anna Alves[e], Cristina Wayne Nogueira[d], Elizandra Braganhol[b,c], Letícia Cruz[a,*]

[a] Laboratório de Tecnologia Farmacêutica, Programa de Pós-graduação em Ciências Farmacêuticas, Centro de Ciências da Saúde, Universidade Federal de Santa Maria, Santa Maria, RS, Brazil
[b] Programa de Pós-Graduação em Biociências, Universidade Federal de Ciências da Saúde, Porto Alegre, RS, Brazil
[c] Programa de Pós-Graduação em Bioquímica e Bioprospecção, Centro de Ciências Químicas, Farmacêuticas e de Alimentos, Universidade Federal de Pelotas, Pelotas, RS, Brazil
[d] Laboratório de Síntese, Reatividade e Avaliação Farmacológica e Toxicológica de Organocalcogênios, Centro de Ciências Naturais e Exatas, Universidade Federal de Santa Maria, Santa Maria, RS, Brazil
[e] Laboratório de Patologia, Departamento de Patologia e de Medicina Legal, Universidade Federal de Ciências da Saúde de Porto Alegre, Porto Alegre, RS, Brazil

ARTICLE INFO

Keywords:
Selenium
Cancer
Polymeric nanoparticles
Glioma

ABSTRACT

Background: Gliomas are the most aggressive malignant tumors of the central nervous system. The diphenyl diselenide [$(PhSe)_2$] is an organoselenium compound that has multiple pharmacological properties. Previous reports showed that $(PhSe)_2$ nanoencapsulation potentiates its *in vitro* antitumoral action and reduces its toxicity.
Objective: In this sense, the current study was designed to further evaluate the $(PhSe)_2$ antitumoral effect by a set of *in vitro* techniques using a glioma cell line as well as by an animal model of gliobastoma.
Methods: For the *in vitro* tests, the cell viability, propidium iodide uptake and nitrite levels of rat glioma C6 cells were determined after incubation with free $(PhSe)_2$ or $(PhSe)_2$-loaded nanocapsules (NC). The glioblastoma model was induced by implantation of C6 glioma cells in the right striatum of rats. Following, animals were submitted to a repeated intragastric administration treatment with $(PhSe)_2$ or NC $(PhSe)_2$ (1 mg/kg/day for 15 days) to assess the possible antitumor effect.
Main findings: Both compound forms decreased the C6 glioma cells viability without causing any effect in astrocytes cells (healthy control). Importantly, the NC $(PhSe)_2$ had superior cytotoxic effect than its free form and increased the nitrite content. Independent of the $(PhSe)_2$ forms, the intragastric treatment reduced brain tumor size and caused neither alteration in the plasma renal and hepatic markers of function nor in the parameters of oxidative balance in brain, liver and kidneys.
Principal conclusions: The $(PhSe)_2$ nanoencapsulation improved its cytotoxic effect against C6 glioma cells and both compound forms attenuated the tumor development.

1. Introduction

Gliomas are a group of aggressive and greatly invasive central nervous system tumors that have high mortality and morbidity rates [1,2]. Among them, the glioblastoma is the ultimate grade of malignancy, in which the median overall survival of patients does not exceed a year after the diagnosis [2,3]. The current available therapy includes a combination of neurosurgical resection, radiotherapy and chemotherapy. However, surgery is not frequently indicated because of high recurrence rate of the tumor, elevate proliferative potential, and a specific infiltrative growth pattern. Besides, the main reason that lead to chemotherapy failure is associated with the difficulty of drugs passing through the blood–brain barrier, which restricts the access of drugs to the central nervous system and induces therapy failure [2,4]. Thus,

* Corresponding author at: Departamento de Farmácia Industrial, Universidade Federal de Santa Maria, Santa Maria, 97105-900, Brazil.
E-mail address: leticiacruz@smail.ufsm.br (L. Cruz).

https://doi.org/10.1016/j.jtemb.2019.06.010
Received 12 March 2019; Received in revised form 9 May 2019; Accepted 14 June 2019

the development of novel and improved pharmacological approaches for glioma treatment is an urgent need.

The diphenyl diselenide [$(PhSe)_2$] is a synthetic organoselenium compound that has multiple pharmacological properties [5]. Of particular importance, the antitumor action of $(PhSe)_2$ was already demonstrated against human neuroblastoma [6], human colon adenocarcinoma [7] and human melanoma cells lines by *in vitro* assessments [8] as well as in a preclinical model of mammary cancer in rats [9]. Converging lines of evidence suggest that the molecular mechanisms of $(PhSe)_2$ antitumoral action could be attributed to the modification of anti-apoptotic and pro-apoptotic proteins content and the expression of p53 gene, which regulates the cells growth cycle rate [7,10]. In this context, Melo and co-workers demonstrated that the MCF-7 cells treatment with $(PhSe)_2$ mitigated the tamoxifen-induced DNA damage without modifying the antitumor effect. The compound incubation did not abolish the selective toxicity of tamoxifen against the MCF-7 cells even avoiding the DNA damage [11]. This evidence reinforces the promising potential of the compound regarding cancers treatment, even as first line and/or adjuvant therapy, or as a protector of cells against secondary damage caused by chemotherapy drugs.

Despite the pharmacological properties of $(PhSe)_2$, some toxic issues limit its therapeutic uses, such as the inhibition of enzymes (δ-aminolevulinate acid dehydratase (δ-ALA-D)) [12] and oxidation of biomolecules [13]. In addition, $(PhSe)_2$ is a poorly water-soluble compound [14], which leads to low oral bioavailability [15] and hinders its administration by other routes, such as the parenteral one. In the context, the $(PhSe)_2$ incorporation into polymeric nanocapsules arises as an alternative to optimize its toxicological and physicochemical limitations as well as maximize pharmacological actions [16,17].

The nanostructured systems have been extensively studied because of the many advantages provided by encapsulating drugs, for instance: i) sustained and site-specific drug delivery [18], ii) stability improvement [19] and iii) toxicity reduction of drugs [18,20] as well as iv) an enhancement in their pharmacological effects [21–23,24]. Despite the great number of scientific reports concerning nanocarriers development focused on cancer management, there are few FDA approved nanomedicines. The main examples are Abraxane (breast cancer), Doxil (ovarian cancer), Oncaspar (acute lymphoblastic leukemia), DaunoXome (Kaposis's sarcoma) and Emend for the chemotherapy-induced nausea. The improvement in the therapeutic effectiveness of such drugs in cancer management could be mainly attributed to site-specific drug release and side effects reduction [25–27].

Some studies regarding $(PhSe)_2$ incorporation into polymeric nanocapsules demonstrated that this association expanded its biological distribution [16] and antioxidant action without causing toxic effects [17]. Recently, our research group developed a formulation of $(PhSe)_2$-loaded nanocapsules that showed many advantages in comparison to the free compound. Despite the adequate physicochemical characteristics, the nanoencapsulation provided superior storage stability and photostability as well as selectively reduced the viability of A375 melanoma cells, without causing toxicity to healthy keratinocyte cells [8]. Furthermore, the zebrafish exposure to $(PhSe)_2$-loaded nanocapsules elicited neither locomotor impairments nor modified the oxidative status of zebrafish brain, suggesting that the compound nanoencapsulation reduced its apparent toxicity [28].

Thus, considering the potential of $(PhSe)_2$-loaded nanocapsules for cancer treatment, the purpose of this study was to investigate the antitumor effect of free and nanoencapsulated $(PhSe)_2$ against the glioblastoma. For this, *in vitro* and *in vivo* sets of experiments were carried out to demonstrate the possible efficacy of the formulation against C6 rat glioma cells and in an animal model of glioblastoma. Besides, an *in vivo* toxicological study was also performed.

2. Materials and methods

2.1. Drugs, reagents and materials

The $(PhSe)_2$ was obtained following a previously described method of Paulmier [29]. Chemical purity of the compound (99.9%) was assessed by gas chromatography-mass spectrometry and high-performance liquid chromatography (Shimadzu QP2010PLUS GC/MS). The ^1H and ^{13}C nuclear magnetic resonance spectra were obtained at 400 MHz (Bruker AvanceTM III HD) and showed analytical and spectroscopic data in full agreement with the assigned structure.

Poly(Ɛ-caprolactone) (PCL) (MW: 80 KDa) and Span 80® (sorbitan monooleate) were acquired from Sigma Aldrich (Brazil). Tween 80® (polysorbate 80) and MCT (medium chain triglycerides) were furnished by Delaware (Brazil). Dulbecco's modified Eagle's medium (DMEM), Fungizone, penicillin/streptomycin, 0.25% trypsin/EDTA solution and fetal bovine serum (FBS) were obtained from Gibco (USA). The 3(4–5-dimethyl)-2-5diphenyl tetrazolium bromide (MTT) was acquired from Thermofisher. The glioma cell line C6 was purchased from American Type Culture Collection (USA). All other chemicals and solvents were obtained from standard commercial suppliers with analytical grade standard and were used as received.

2.2. Nanocapsules suspensions

Nanocapsules suspension containing $(PhSe)_2$ were prepared and characterized (average diameter, polydispersity index, zeta potential, pH, $(PhSe)_2$ content and encapsulation efficiency) as described in our previous study [8]. Briefly, an organic phase containing PCL (0.1 g), Span 80® (0.077 g), MCT (330 μL), acetone (27 mL), and $(PhSe)_2$ (0.05 g) was magnetically stirred at 40 °C for 60 min and then injected into a Tween 80® aqueous dispersion (0.077 g; 53 mL). The mixture was magnetically stirred for 10 min longer at room temperature and then solvent was eliminated by evaporation under reduced pressure until a 10 mL of final volume, which corresponds to a $(PhSe)_2$ concentration of 5.0 mg/mL (NC $(PhSe)_2$). For comparison purposes, formulations without $(PhSe)_2$ were also prepared (NC B).

2.3. In vitro assays

2.3.1. Glioma cultures

The C6 cells were cultured in DMEM containing 0.1% Fungizone and 100 U/L penicillin/streptomycin and supplemented with 5% FBS (v/v). After the cultures reached confluency, the cells were released by trypsinization and seeded in 96 well plates, which were maintained at 37 °C in a humidified atmosphere of 5% CO_2 for 24 h. The plates containing C6 cells were incubated with NC $(PhSe)_2$ or free $(PhSe)_2$ at the concentrations 1, 2.5, 5, 10, 25, 50, 100 and 200 μM for 48 h. These concentrations were selected based on our previous study concerning the cytotoxic effect of $(PhSe)_2$ [8]. To achieve such concentrations, 10-fold serial dilutions were made using DMEM culture medium from the $(PhSe)_2$ nanocapsules suspension or the stock solution of free $(PhSe)_2$, which was dissolved in DMSO (10%). For comparison purposes, plates incubated with DMSO (10%) or NC B were simultaneously performed. All observations were validated by at least three independent experiments and for each experiment the analyses were conducted in triplicate.

2.3.2. Primary astrocyte cultures

Primary astrocyte cultures were prepared as described by da Silveira and coworkers [26]. Briefly, brain cortex samples of newborn Wistar rats (1–2 days old; Ethical committee protocol number 23110009402/2016-01) were obtained, removed and mechanically homogenized in a Ca þ 2 and Mg þ 2 free balanced salt solution pH 7.4, (137 mM NaCl, 5.36 mM KCl, 0.27 mM Na_2HPO_4, 1.1 mM KH_2PO_4 and 6.1 mM glucose). After centrifugation (5 min/1000 *xg*), the pellet was suspended in

DMEM supplemented with 10% FBS. The cells (5×10^4) were plated in poly-L-lysine-coated 96-well plates and 4 h later they were shaken, washed with PBS, and the medium was changed to remove neuron and microglia contaminants. Over a period of 20–25 days, the cultures grew until achieve confluence and the medium was replaced every four days. The plates containing astrocytes cells were incubated with NC $(PhSe)_2$ or free $(PhSe)_2$ at a concentration range 10, 25, 50 and 100 μM for 48 h. Cells treated with DMSO (10%) or NC B were used for comparison purposes as described in section 2.3.1.

2.3.3. MTT assay

The MTT reduction assay was performed to determine the C6 and astrocytes viability. The test was carried out according to our previous study [8]. After the aforementioned incubations, the plates were washed twice with sodium phosphate buffer and the yellow tetrazolium salt MTT solution (1 mg/mL) was added to the plates. Following, the plates were incubated at 37 °C for 3 h, under light protection until the formation of violet formazan crystals. Later, the solution was then removed and an aliquot of DMSO was added to each well. The optical density was measured at 492 nm and the results were expressed as cell viability (%) in comparison to the DMEM culture medium, which was used as the negative cell death control.

2.3.4. Nitrite content determination

The Griess reaction was used to estimate the nitrite (NO_2^-) levels in the culture medium [30] after C6 incubation with $(PhSe)_2$, free and nanoencapsulated. Briefly, culture supernatant was mixed with sulfanilamide in 5% phosphoric acid, followed by an incubation at room temperature during 10 min. Then, n-1l-napthylethylenediamine (NED) 0.1% was added to the samples and incubated protected from light for 10 min longer. The absorbance was determined in a spectrophotometer at 540 nm. The amount of nitrite in the supernatant was estimated using a sodium nitrate standard curve. Results were expressed as μM of NO_2^-.

2.3.5. Propidium iodide assay

Cell damage in C6 cells was assessed by fluorescent imaging of propidium iodide (PI) uptake. After the incubations, cells were washed with calcium - magnesium free (CMF) and incubated with a PI solution (7.5 μM) for 1 h. PI fluorescence was excited at 515-560 nm using an inverted microscope (Olympus IX71, Japan) equipped with a standard rhodamine filter. The images were captured using a digital camera connected to the microscope and the PI positive cells were counted. The results were expressed as the quantity of positive PI cells per field.

2.4. Animals

The *in vivo* experiments were carried out using male adult Wistar rats (250–350 g), which were maintained in an appropriated accommodation room under the following conditions: controlled temperature (25 ± 2 °C) and relative humidity (60%), suitable brightness, soundproofing, under a 12:12 h light/dark cycle (7 AM to 7 PM) and with free access to water and food (GUABI, Brazil). The experimental procedures were approved by the Ethical Research Committee of Federal University of Santa Maria (toxicological evaluations - protocol number 2171170217/2017) and Ethical Research Committee of the Federal University of Pelotas (animal model of glioma - protocol number: 23110009402/2016-01) affiliated to the Council for Control of Animal Experiments (CONCEA) and in accordance with the NIH Guide for the Care and Use of Laboratory Animals.

2.5. In vivo toxicity

2.5.1. General procedures and treatments

The animals were randomly distributed in four groups (n = 5–6 animals/group) and received the treatment by intragastric route (i.g; 1 mL/Kg of body weight), once a day, for 15 days (Fig. 1A). The experimental groups were the following:

I) Control - the animals received MCT (1 mL/Kg, i.g.);

II) NC B - the animals received NC B suspension (1 mL/Kg, i.g.);

III) $(PhSe)_2$ - the animals received $(PhSe)_2$ at 5 mg/Kg (1 mL/Kg, i.g.);

IV) NC $(PhSe)_2$ - the animals received NC $(PhSe)_2$ at 5 mg/Kg (1 mL/kg, i.g.).

The free compound was dissolved in MCT (5 mg/mL) and the formulations (NC $(PhSe)_2$ and NC B) were prepared as described in section 2.3. To rationally select a compound dose that would be used in the *in vivo* experiments we performed a detailed evaluation of the scientific literature concerning the $(PhSe)_2$ pharmacological and toxicological properties [5,13]. Based on such survey, we selected a (PhSe) dosage that elicited other important pharmacological actions (5 mg/Kg), such as antinociceptive, antioxidant and anti-inflammatory [13]. The animals were periodically monitored every 24 h to record mortality, behavioral pattern changes, ptosis, tremors, diarrhea, salivation, piloerection, tremors, locomotor alterations or seizures. Furthermore, before receiving the treatment, the body weight gain and food consumption were daily recorded as well.

2.5.2. Toxicological parameters

Twenty-four hours after the last treatment, the animals were slightly anesthetized prior to blood collection by heart puncture. In sequence, blood samples were centrifuged at 2500 *xg* during 10 min to obtain the plasma fraction, which were used for determining biochemical markers of hepatic and renal function. After this procedure, rats were sacrificed and samples of brain, liver and kidneys were collected and *in situ* macroscopically observed based on their position, color, shape, size and consistency. Following, the samples were accurately weighed, frozen and stored at -80 °C until the biochemical analysis.

2.5.2.1. Plasma biochemical parameters. The plasma samples were used to estimate hepatic and renal functionality using commercial kits (Labtest, Brazil). The total bilirubin levels, alanine (ALT) and aspartate aminotransferase (AST) activities were measured to evaluate hepatic function while urea and creatinine levels were used to assess renal function.

2.5.2.2. Tissue preparation and biochemical assays. The tissue samples were homogenized in 50 mM Tris HCl at pH 7.4, 1:5 (brain) or 1:10 (liver and kidneys) (w/v), and then centrifuged at 2500 *xg* during 10 min at 4 °C to yield a low-speed supernatant fraction (S_1). Freshly prepared S_1 was used to estimate some parameters of oxidative status. A different protocol of homogenization was conducted to estimate the protein carbonylation level, in which no centrifugation was performed (Section 2.5.2.2.2*)*. Protein concentration was measured by the Bradford methodology [31], using bovine serum albumin (1 mg/mL) as the analytical standard.

2.5.2.2.1. Non-protein thiol levels. To determine the non-protein thiol (NPSH), an aliquot of S_1 was mixed with 10% trichloroacetic acid solution (1:1, v/v) and the clear supernatant (S_2) was obtained through centrifugation. The S_2 contains the free thiol groups, which reacts with 5,5- dithiobis (2-nitrobenzoic acid) (DTNB) generating a yellow complex measured at 412 nm [32]. The results were expressed as nmol NPSH/g tissue.

2.5.2.2.2. Protein carbonylation. Briefly, homogenates were diluted 1:8 (v/v) and an aliquot was added to the reaction mixture containing 10 mM DNPH (prepared in 2 M HCl). The samples were protected from light and shaken with a vortex mixer each 15 min over 1 h. Following, denaturation buffer, ethanol and hexane were added to each tube. The tubes were shaken with a vortex mixer for 40 s and centrifuged (15 min). The supernatants were discarded and the pellets were washed twice with ethanol:ethyl acetate (1:1, v/v) and resuspended in a denaturation buffer. The sample tubes were shaken with a vortex mixer for 5 min. These samples were used to measure absorbance at

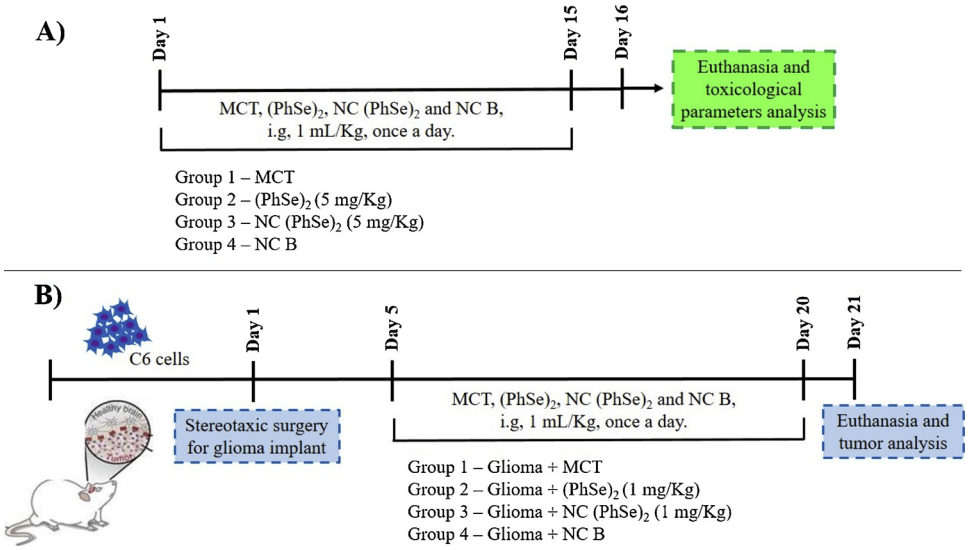

Fig. 1. Schematic representation of the experimental design performed to evaluate toxicity (A) and antiglioma effect (B). The animals received during fifteen days a daily administration of $(PhSe)_2$, free or incorporated into NCs suspension, and the vehicles, MCT or NC B. For notes, i.g means intragastric route; $(PhSe)_2$ means free diphenyl diselenide; NC $(PhSe)_2$ means nanocapsules containing diphenyl diselenide; NC B means nanocapsules without $(PhSe)_2$; and MCT means medium chain triglycerides.

370 nm [33]. The results were reported as carbonyl content (nmol/mg protein).

2.5.2.2.3. Delta-aminolevulinic acid dehydratase (δ-ALA-D) activity. The δ-ALA-D activity was determined according to Sassa [34]. The samples were incubated at 37 °C in a medium containing 45 mM phosphate buffer, pH 6.8 and the enzymatic reaction was initiated by adding the substrate (5-aminolevulinate) to a 2.2 mM final concentration. The incubation was stopped by adding trichloroacetic acid solution (10% TCA) with 10 mM $HgCl_2$. The reaction product, porphobilinogen, was spectrophotometrically measured at 555 nm with modified Erlich's reagent. The results were expressed as nmol of porphobilinogen /h/mg protein.

2.5.2.2.4. Superoxide dismutase (SOD) activity. SOD activity was determined as described by Misra and Fridovich [35]. Prior diluted aliquots of S_1 (1:10 v/v) were added in a Na_2CO_3 buffer 50 mM pH 10.3 and the enzymatic reaction was initiated by adding epinephrine. The color reaction was measured at 480 nm and the enzyme activity was expressed as U (1U decomposes 1 µmol of H_2O_2/min at pH 7 and at 25 °C)/mg protein.

2.5.2.2.5. Glutathione-S-Transferase (GST) activity. The assay to determine the GST activity was performed based on Habig and coworkers [36]. The reaction mixture contained an aliquot of S_1, 0.1 M potassium phosphate buffer pH 7.4, 100 mM GSH and as substrate 100 mM 1-chloro-2,4 dinitrobenzene (CDNB) were used. The reaction product was spectrophotometrically detected at 340 nm and the results were expressed as CDNB conjugated nmol/minute/mg protein.

2.5.2.2.6. Catalase (CAT) activity. The CAT activity was carried out by monitoring the H_2O_2 consumption at 240 nm. The enzymatic reaction was performed by adding an aliquot of S_1 and the substrate (H_2O_2) at a concentration of 0.3 mM in a medium containing 50 mM phosphate buffer, pH 7.0. The enzymatic activity was expressed in units (1U decomposes 1 µmol of H_2O_2/min at pH 7 and at 25 °C)/mg protein [37].

2.5.2.2.7. Reactive species (RS) production. The substrate 2′-7′-dichlorofluorescein diacetate (DCFH-DA) was applied to measure the intracellular formation of ROS, according to Myhre and co-workers [38]. An aliquot of S_1 was mixed with DCFH-DA (1 mM) and Tris – HCl buffer (10 mM; pH 7.4) and then incubated for 60 min protected from light. The fluorescence was measured using a fluorimeter (488 nm for excitation and 525 nm for emission) and ROS levels were expressed as nmol of DCF/ mg protein.

2.6. Preclinical model of glioblastoma

2.6.1. Glioma implantation

The rats were anesthetized with ketamine and xylazine injected by the intraperitoneal route. Then, a total of 1×10^6 C6 cells were dispersed in DMEM and an aliquot (3 µL) was injected in the right striatum at a depth of 6.0 mm (coordinates regarding bregma: 0.5 mm posterior and 3.0 mm lateral) of animals [26]. The C6 glioma cells were cultured as described at Section 2.3.1. Immediately after surgery, the animals were kept in a warm room until full recovery from the anesthesia.

2.6.2. General procedures and treatments

Five days after glioma implantation, the rats were randomly assigned to different groups (4–5 animals/group), each one receiving the following treatments once a day, for 15 days by the intragastric route (Fig. 1B):

I) Control - the animals received MCT (1 mL/Kg, i.g.);

II) NC B - the animals received NC B suspension (1 mL/Kg, i.g.);

III) $(PhSe)_2$ - the animals received $(PhSe)_2$ at 1 mg/Kg (1 mL/Kg, i.g.);

IV) NC $(PhSe)_2$ - the animals received NC $(PhSe)_2$ at 1 mg/Kg (1 mL/Kg, i.g.).

In comparison to the protocol of toxicological evaluation (Section 2.5), a lower $(PhSe)_2$ dose was selected to perform the treatment of the animals in the glioblastoma model [5,13]. The tumor implantation can induce an intense systemic inflammatory process, which could modify the immune system and the metabolic processes of the animals. Thus, based on the results obtained in the toxicological evaluation and our pilot experiments, the dose of 1 mg/Kg was selected to evaluate the antitumor effect in the *in vivo* model. The free compound form was dissolved in MCT (1 mg/mL). The NC $(PhSe)_2$ and NC B were prepared as described in Section 2.3 and diluted with sterile water to achieve the desired concentration (1 mg/mL). After 20 days after glioma implantation (5 days after glioma implantation + 15 days of treatment), the rats were euthanized and the entire brain was removed, sectioned and fixed with 10% paraformaldehyde (pH 7.4) to further evaluation.

2.6.3. Tumor size quantification

Tumor size was analyzed using captured images with Image Tool Software. The total volume (mm^3) of the tumor was computed by summing the segmented areas and by multiplication of the slice resolution. At least five sections (2–3 µm thick, paraffin embedded and stained with Hematoxylin & Eosin) from each animal of NC B and NC $(PhSe)_2$ groups were analyzed by a pathologist that was blinded

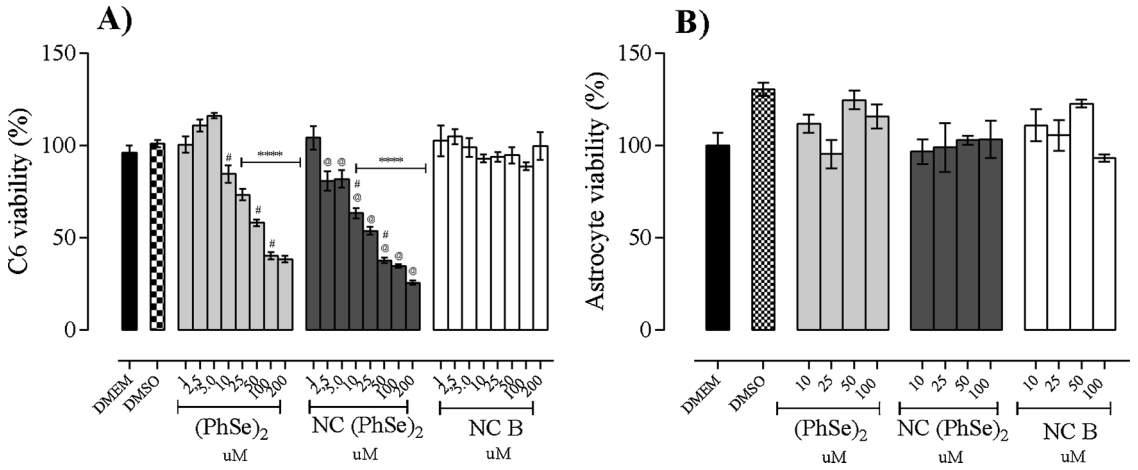

Fig. 2. Cytotoxic effect of NC $(PhSe)_2$ and free $(PhSe)_2$ against glioma cell line (C6) (A) and in primary astrocyte cells (B) after 48 h of incubation assessed by MTT assay. Each column represents the mean ± S.E.M. of triplicate. Asterisks denote significant differences (**** $p < 0.0001$) in comparison to the negative control group and sharps ($^{\#}$ $p < 0.05$) denote significant differences among the concentrations of the same group, by one-way ANOVA, followed by Tukey's post hoc test. Arroba symbol ($^{@}$ $p < 0.05$) denotes significant differences between the same concentrations of free $(PhSe)_2$ and NC $(PhSe)_2$ by Unpaired Student's *t* test.

concerning the treatments.

2.7. Statistical analysis

All experimental results are presented as mean (s) ± standard error of the *n* observation means (S.E.M.). Data normality was assessed using D'Agostino and Person omnibus normality test. The GraphPad Prism® version 6 software was used to calculate IC_{50} values (linear regression) and the statistical evaluation, which was performed by Student's *t* test and one-way analyses of variance (ANOVA) followed by post-hoc Tukey's test. Values of $p < 0.05$ were considered statistically significant.

3. Results

3.1. In vitro assays

3.1.1. Evaluation of C6 cells viability

The $(PhSe)_2$ *in vitro* antiglioma effect was investigated employing MTT test (Fig. 2A). The free $(PhSe)_2$ significantly reduced the C6 viability at the concentration range 25–200 μM (73.30, 58.12, 40.27 and 38.27%, respectively) while NC $(PhSe)_2$ was effective in reducing cell viability at lower concentrations than free $(PhSe)_2$ (10 μM to 200 μM; 63.23, 53.69, 37.72, 34.66 and 25.60%, respectively). The statistical evaluation revealed significant difference between $(PhSe)_2$ free and nanoencapsulated, indicating that NC $(PhSe)_2$ had a superior effect against C6 cell line. Reinforcing these results, the free $(PhSe)_2$ presented an IC_{50} value of 74.83 μM, while NC $(PhSe)_2$ was 43.40 μM. The NC B had no antitumor effect independent of the concentration tested.

3.1.2. Evaluation of astrocyte cells viability

The astrocytes cells were used as non-transformed cell model to assess the formulations safety and selectivity (10–100 μM; Fig. 2B). After 48 h of incubation, no significant differences in the cell viability were observed among the experimental groups. All samples and concentrations tested did not significantly modify the cell viability ($p > 0.05$).

3.1.3. Nitrite content determination in C6 cells

Concerning to the nitrite levels determination, our data demonstrated that the incubation with NC $(PhSe)_2$ and NC B (50, 100 and 200 μM) significantly increased the nitrite content (Fig. 3). Interestingly, free $(PhSe)_2$ did not modify the nitrite content.

3.1.4. Propidium incorporation in C6 cells

The possible occurrence of necrosis induced by the treatment was evaluated using the PI incorporation in C6 cells. Corroborating with the MTT assay, the incubation of C6 cells with free $(PhSe)_2$ and NC $(PhSe)_2$ at 100 μM caused cell morphological alterations and density reduction (Fig. 4A). No modifications were observed in C6 cells incubated with NC B. In addition, the number of positive PI cells was higher in the cells incubated with NC $(PhSe)_2$ (10.5 ± 1.4 positive cells). The statistical evaluation revealed that there is a significant difference of NC $(PhSe)_2$ group in comparison to the other groups ($p < 0.05$) (Fig. 4**B**).

3.2. In vivo toxicological evaluation

Independent of the treatment, the repeated administration schedule triggered no clinical abnormality signs or death to the animals over the experimental protocol. Neither the relative body weight gain (Fig. 5A) nor the total food consumption (Fig. 5B) showed statistical difference among the groups that received the $(PhSe)_2$, free or nanoencapsulated, and MCT oil. On the other hand, the animals treated with NC B had an increase in food consumption and consequently presented an augmentation in the relative body weight over the days. The samples of brain, liver and kidneys of the treated animals presented similar morphology, color, shape, size and consistency (*Data not shown*).

Table 1 demonstrates the results of plasma biochemical parameters. No statistical difference was detected neither to AST and ALT activities nor to total bilirubin, creatinine and urea levels ($p > 0.05$ by One-way ANOVA). In addition, the repeated treatment schedule did not modify the levels of NPSH, ROS, and carbonyl protein as well as δ- ALA-D, SOD, GST, and CAT activities ($p > 0.05$ by One-way ANOVA; Fig. 6).

3.3. Antiglioma action in a preclinical model

The effectiveness of the treatments was evaluated by the analysis of tumor size (Fig. 7A). The implanted tumors had glioblastoma characteristics and $(PhSe)_2$, free or nanoencapsulated, were effective in reducing tumor progression. The One-Way ANOVA analysis showed a significant reduction in tumor size in the groups treated with $(PhSe)_2$, free (13.94 ± 3.05 mm^3) or nanoencapsulated (15.49 ± 5.32 mm^3), in comparison to the group treated with MCT oil (176.60 ± 22.91 mm^3) ($p < 0.0001$) or NC B (112.20 ± 19.93 mm^3) ($p < 0.005$). Reinforcing these data, Fig. 7**B** displays the representative brain images of the animals treated with NC B or NC $(PhSe)_2$. The administration of NC $(PhSe)_2$ mitigated the tumor development in comparison to NC B. The histopathological evaluation demonstrated that at the site of glioma

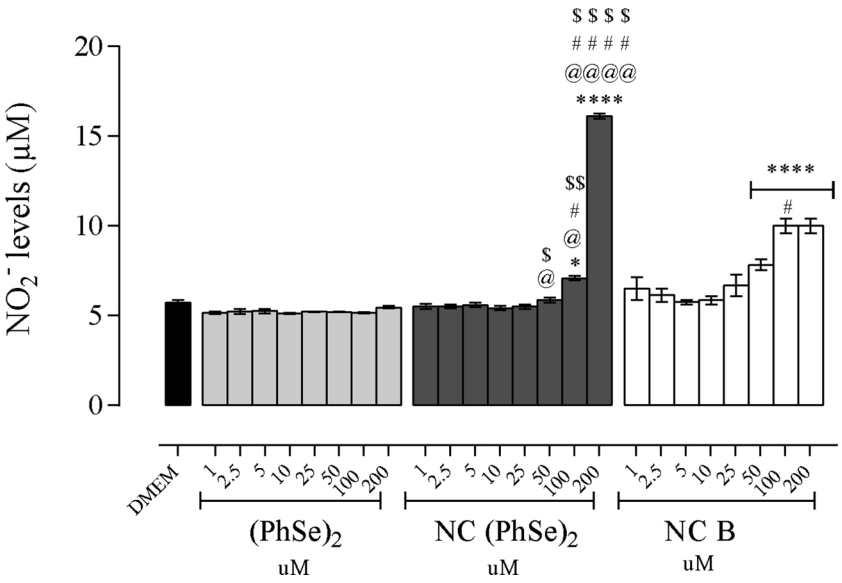

Fig. 3. Nitrite (NO_2^-) levels in C6 cell cultures. Each column represents the mean ± S.E.M. of triplicate. Asterisks denote significant differences (* $p < 0.005$ and **** $p < 0.0001$) in comparison to the negative control group and sharps ($^{\#}$ $p < 0.05$ and $^{\#\#\#\#}$ $p < 0.0001$) denote the differences among the concentrations in the same group, by one-way ANOVA, followed by Tukey's post hoc test. Arroba symbol ($^{@}$ $p < 0.05$ and $^{@@@@}$ $p < 0.0001$) denotes significant differences between the same concentrations of NC $(PhSe)_2$ and $(PhSe)_2$ while cipher ($^{\$}$ $p < 0.05$, $^{\$\$}$ $p < 0.01$, and $^{\$\$\$\$}$ $p < 0.0001$) means significant differences between the same concentrations of NC B and NC $(PhSe)_2$ by Unpaired Student's *t* test.

cells implantation it was observed characteristics of a residual tumor, with a reduction in coagulative necrosis, intratumoral hemorrhage, lymphocytic infiltration, peritumoral edema, and microvascular proliferation in the group of animals treated with NC $(PhSe)_2$.

4. Discussion

Despite the $(PhSe)_2$ pharmacological potentialities, its clinical use remains a challenge due to its physicochemical and toxic issues [12,15]. In this sense, the $(PhSe)_2$ incorporation into nanocapsules emerges as an

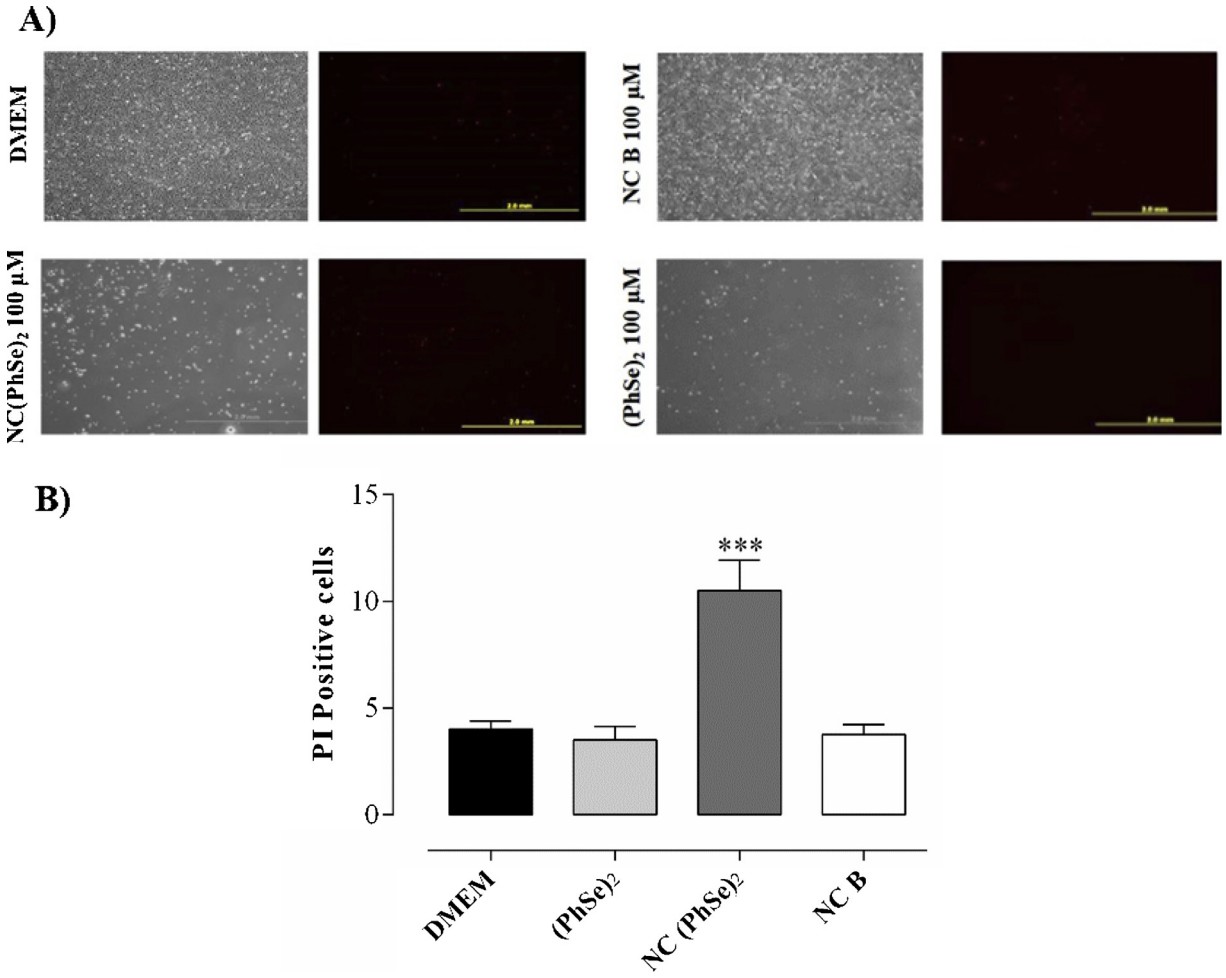

Fig. 4. Propidium iodide (PI) incorporation in C6 cell following 48 h of incubation with $(PhSe)_2$, free or nanoencapsulated: A) microscopic images and B) number of PI positive cells. Asterisks denote significant differences ($^{***}p < 0.001$) in comparison to the other groups, by one-way ANOVA, followed by Tukey's post hoc test.

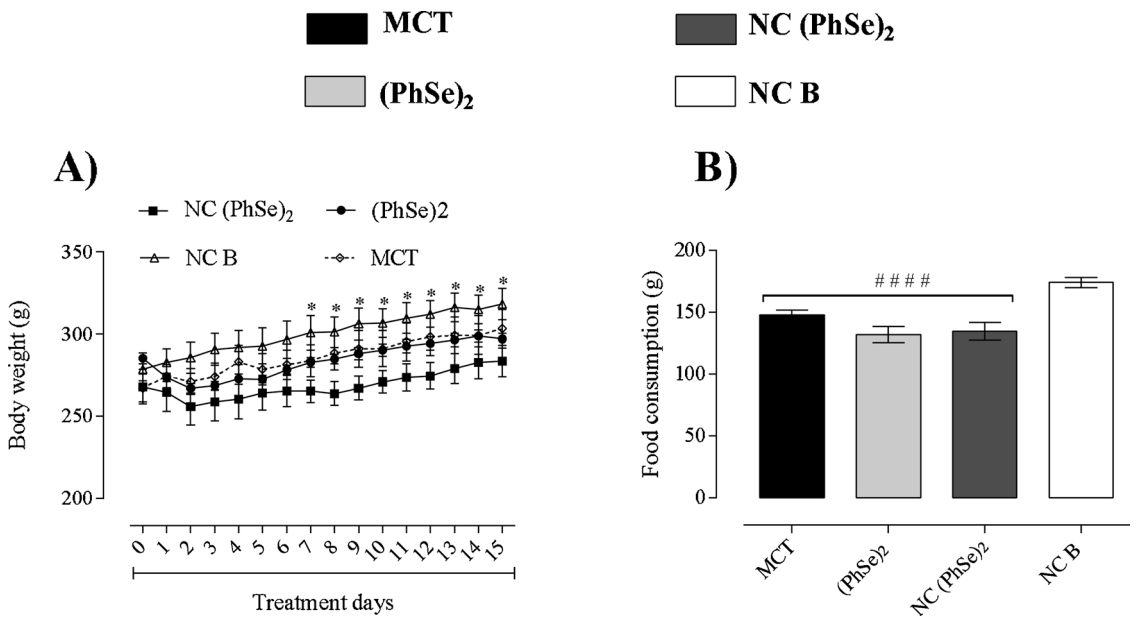

Fig. 5. Effect of the repeated treatment in body weight gain **(A)** and food intake **(B)** over the experimental protocol. Each column/point represents the mean ± S.E.M of 5–6 rats/group. The One-way ANOVA followed by Tukey's post hoc test was used for statistical evaluation. Asterisks denote statistically significant differences of NC B groups in comparison to the other groups ($^{*}p < 0.05$); sharps denote statistically differences among the group treated with NC B in comparison to the other groups ($^{\#\#\#\#}$ p < 0.0001).

advantageous alternative to improve its therapeutic index and optimize the treatment regimen by expanding the array of possible administration routes. The results obtained in the current study demonstrated the effectiveness of $(PhSe)_2$, free and nanoencapsulated, against glioblastoma multiforme using *in vitro* and *in vivo* protocols. In addition, the repeated administration showed neither unspecific toxic effects nor oxidative balance impairment, suggesting the safeness of the treatment.

According to World Health Organization (WHO), gliomas are classified in astrocytic tumors grade II and III, oligodendrogliomas grade II and III and glioblastomas as grade IV, which are the most aggressive kind [39]. Despite the multimodality approach to glioma treatment, the patients had a survival rate between 3 and 16 months [40]. In this scenario, the nanocarrier systems can be a promising alternative regarding innovative and improved therapies for glioma treatment [4,26,41,42]. The development of nanotechnological-based therapies to glioblastoma treatment could increase the quantity of drug that reaches the central nervous system because of the small size of the nanoparticles. Besides, the nanocarriers can promote a controlled release of the active, which improves its efficacy and reduces the toxic effects in other organs [42,43].

Initially, the $(PhSe)_2$ antiglioma effect was assessed using a set of *in vitro* techniques. The results of MTT assay showed that both compound forms selectively reduced C6 cell viability without causing any alteration in astrocyte cells viability. Corroborating with this test, the C6 cell density was also reduced by the treatment with the compound at 100μM concentration. It is important to highlight that the $(PhSe)_2$ nanoencapsulation enhanced the compound antiglioma effect. At some concentrations in which the free compound had no action the NC $(PhSe)_2$ caused a reduction in C6 cells viability, which was further confirmed by the IC_{50} values. Indeed, in our previous study, the $(PhSe)_2$ nanoencapsulation selectively reduced the cell viability of a melanoma cell line (A375), abolishing the cytotoxicity in human keratinocytes [8]. These results are in accordance with other scientific reports that showed an improvement of *in vitro* and *in vivo* biological effects of compounds by associating them into nanocarrier systems [19,22,44,45].

Nitric oxide (NO) is an inorganic free radical, which plays an important and complex role in cancer pathophysiology. It modulates different cellular events dependent on its concentration, such as proliferation, apoptosis, angiogenesis, migration and invasion [46,47]. In gliomas, the NO produced could increase the tumor endothelium permeability, enhancing the delivery of chemotherapeutic drugs [48]. In this sense, our results demonstrated an increase in NO_2^- levels at the highest concentration tested of NC $(PhSe)_2$ and NC B. Of particular importance, it was already reported that the antitumor effect of substances incorporated into nanocapsules composed of PCL and MCT seems to be associated to an increase in the NO production. Drewes and co-workers obtained an augmentation in NO_2^- levels without causing toxicity to tumor cells after cells incubation with blank nanocapsules. However, the high NO_2- levels were linked to the acetyleugenol-loaded

Table 1
Biochemical plasma analyses of animals submitted to the repeated treatment with $(PhSe)_2$ (5 mg/kg, i.g.), free or NC.

Biochemical parameters				
Parameter	MCT	$(PhSe)_2$	NC $(PhSe)_2$	NC B
AST (U/L)	105.30 ± 21.27	99.43 ± 22.74	98.00 ± 17.40	102.9 ± 27.45
ALT (U/L)	94.00 ± 39.22	108.0 ± 46.43	107.6 ± 39.02	145.5 ± 33.67
Total Bilirubin (mg/dL)	0.420 ± 0.220	0.400 ± 0.220	0.480 ± 0.150	0.270 ± 0.050
Creatinine (mg/dL)	0.620 ± 0.300	0.570 ± 0.190	0.520 ± 0.120	0.550 ± 0.110
Urea (mg/dL)	81.13 ± 20.11	96.92 ± 40.13	93.81 ± 29.31	85.57 ± 34.27

Values are expressed as mean ± S.E.M of 5–6 animals/group to each parameter. Data were evaluated through ordinary One-way ANOVA ($p > 0.05$). Abbreviations: AST-aspartate aminotransferase; ALT - alanine aminotransferase; MCT - medium chain triglycerides.

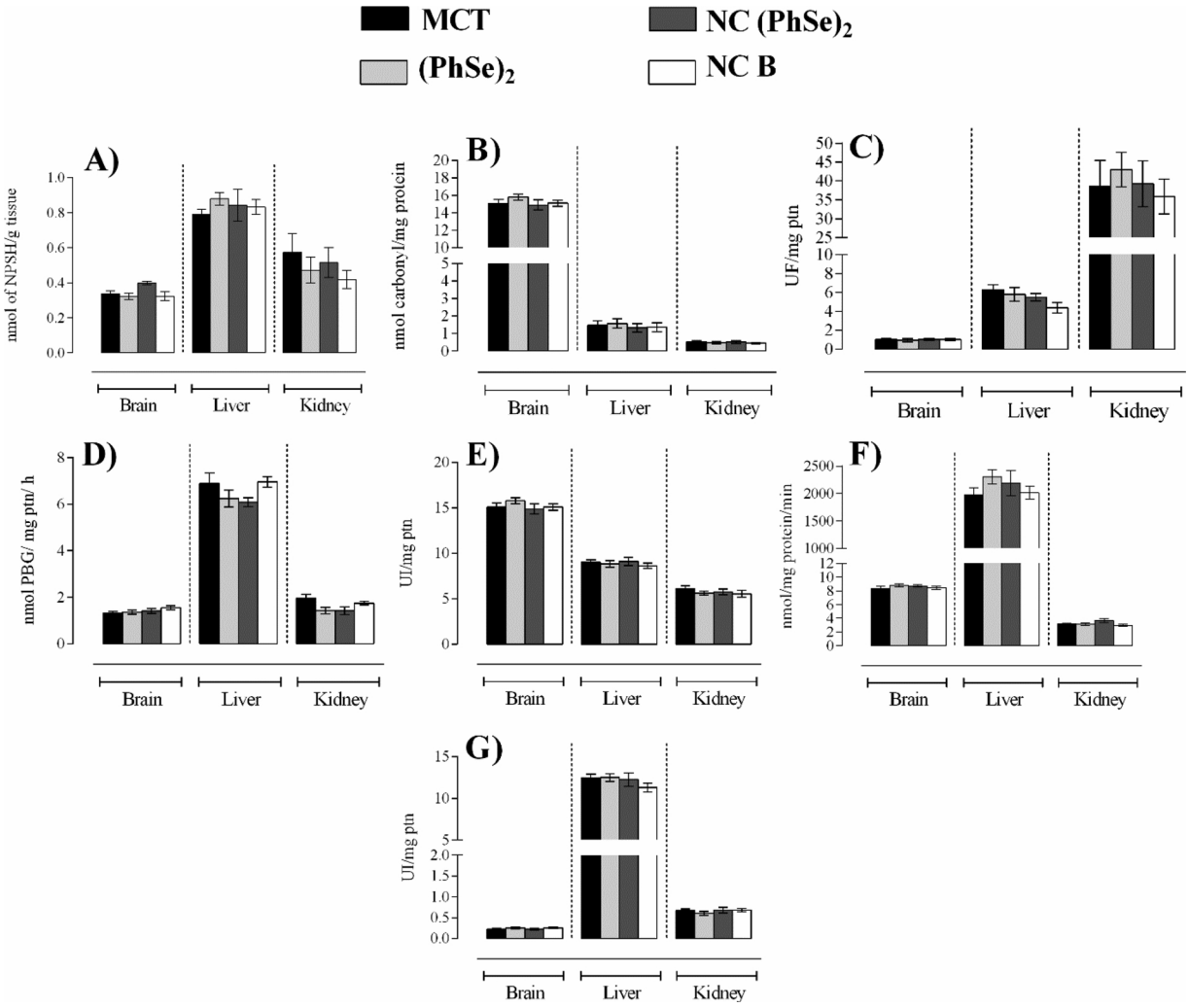

Fig. 6. Effect of the repeated treatment with $(PhSe)_2$ (5 mg/kg, i.g.), free or incorporated into the NC, in the NPSH (A), Carbonyl protein (B) and ROS (C) levels and δ-ALA-D (D), SOD (E) and GST (F) and CAT (G) activity in different tissues. Each column represents the mean ± S.E.M of 5–6 rats/group. Data were analyzed by One-way ANOVA ($p > 0.05$).

lipid core nanocapsules antitumor effect, suggesting that this cellular mediator has an important contribution to the final pharmacological effect [49].

In addition, other mechanisms could be associated with the anti-glioma effect, such as the apoptosis and necrosis pathways. In this study, the PI incorporation assay was used to further investigate the mechanisms through $(PhSe)_2$ exerts its cytotoxicity. The late apoptotic stage and necrotic cells can be identified by the PI incorporation, because of their membrane loss the integrity, thus PI can be uptaked and bind to nuclear DNA, staining the cells [50,51]. In our study, few cells incorporated the PI, suggesting that necrosis is poorly involved in the antiglioma effect of $(PhSe)_2$ and other cell death pathways may mediate such effect. In fact, converging lines of evidence showed that $(PhSe)_2$ promotes its antitumor effect by distinct molecular pathways, such as the modulation of p53 gene expression, regulation of oxidative balance and modification in the ratio of pro-apoptotic and anti-apoptotic proteins [6,7,10,11]. Thus, it is possible to suggest that multiple targets are implicated in the $(PhSe)_2$ antitumoral effect. According to the literature, compounds with antiproliferative effects in tumor cells without promoting a necrotic cell death are considered good candidate as anticancer drugs [52].

Despite the attractive properties of nanosystems, there are some concerns about the biological safety of these formulations/materials. Thus, estimating the possible biological interactions among the nanocapsule with the body and the potential inherent risks of these carriers are critical issues [53]. Besides, depending on the vehicle and administration route, the $(PhSe)_2$ can trigger toxicological impairments [54]. The study of *in vivo* toxicity demonstrated that independent of $(PhSe)_2$ form, the repeated administration schedule did not trigger mortality or systemic toxicity. The evaluation of oxidative status of different tissues (brain, liver and kidneys) showed no alterations as well as the plasma markers of hepatic and renal function, which was also reported to nanocapsules containing *p,p'*- methoxyl-diphenyl diselenide, an organoselenium compound counterpart of $(PhSe)_2$ [55]. Corroborating these results, we recently demonstrated that the nanoencapsulation reduced the apparent $(PhSe)_2$ toxicity and potentiates the compound anxiolytic action in zebrafish [28], broadening the perspective of its therapeutic application.

The literature reports several studies about the $(PhSe)_2$ *in vivo* pharmacological actions, including the anticancer effect [5]. However, this is the first study that evaluated the $(PhSe)_2$ effectiveness in a preclinical model of glioblastoma. The results showed that both $(PhSe)_2$ forms effectively mitigated the tumor growth, reducing the final volume to around 15 mm^3. Besides, the animals treated with NC $(PhSe)_2$ has residual glioma cells implantation. The most common chemotherapeutic drugs used to treat gliomas are carmustine, PCV (procarbazine, lomustine, and vincristine) and the first-line temozolomide [56]. In a study using the same preclinical glioma model, the temozolomide

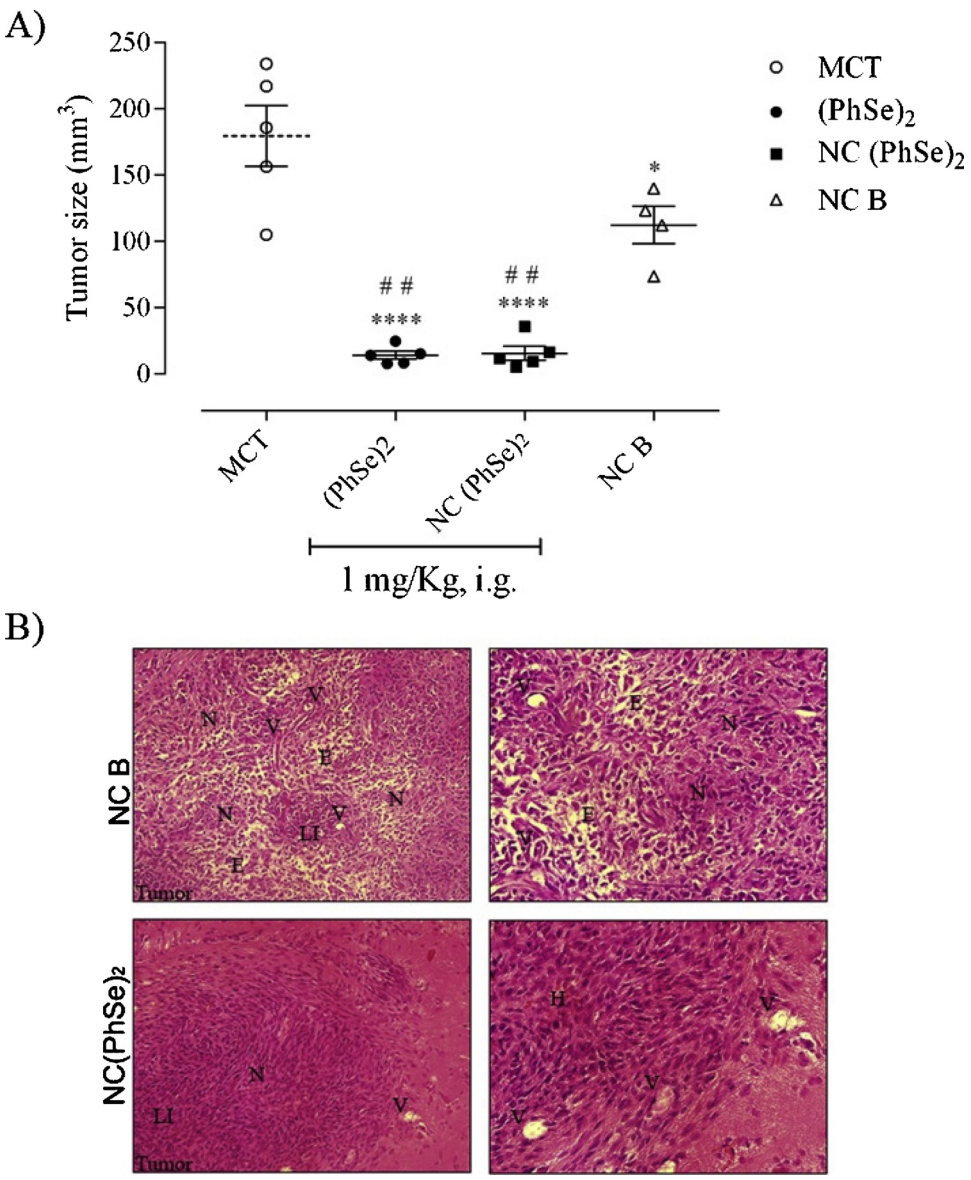

Fig. 7. (A) Effect of repeated treatment in tumor size in glioma-implanted rats. Data were analyzed by one-way ANOVA, followed by Tukey's post hoc test, in which the asterisks denote significant differences (* $p < 0.005$ and **** $p < 0.0001$) in comparison to the MCT oil group and sharps ($^{\#}$ $^{\#}$ $p < 0.01$) means significant differences between $(PhSe)_2$ or NC $(PhSe)_2$ with NC B. **(B)** Representative micrographs of implanted tumors. The sections of implanted rat glioma were stained with hematoxylin and eosin (HE). Representative pictures of histological characteristics that define glioblastoma, as seen in rats implanted with gliomas and treated with unloaded-drug nanocapsule (NC B - upper panel) or treated with $(PhSe)_2$-loaded nanocapsules (NC$(PhSe)_2$ - down panel). **Abbreviation:** Necrosis (N), microvascular proliferation (V), edema (E), Hemorrhage (H), Lymphocytic infiltrate (LI) were observed. (20x magnification - left panel; 40x magnification - right panel).

administration reduced the tumor size to 35 – 30 mm^3 [57]. In this sense, it is possible to suggest that $(PhSe)_2$ has a high efficacy regarding glioma management, however, complementary analyses must be carried out to reinforce such hypothesis. Lastly, it is important to highlight that the nanoencapsulation maintained the antitumor effect of $(PhSe)_2$ without causing any toxicity. Although the pharmacological performance was similar to the free compound, the nanocapsules suspension is a suitable pharmaceutical formulation. Differently from the $(PhSe)_2$ oily solution, the nanoencapsulation of the compound enables its administration by different routes, including the oral and parenteral ones, broadening the perspective of its therapeutic application. Finally, it is important to highlight that the selenium-containing organic molecules do not release the selenium atom even after its biotransformation because of the highly stable covalent bound of the carbon atoms. In the biological systems, the organoselenium compounds act as drugs and probably exert their effects through interactions with the organism and do not serve as a selenium microelement source/supplementation.

5. Conclusion

This study reported the $(PhSe)_2$ effectiveness against glioma tumor using *in vitro* techniques and a preclinical glioblastoma model. The $(PhSe)_2$ nanoencapsulation increased its *in vitro* antitumor effect, which seems to be mediated at least in part by NO pathways without involvement of necrosis mechanisms. Furthermore, the repeated administration of both $(PhSe)_2$ forms mitigated the glioblastoma growth, but future studies are needed to better elucidate the mechanism associated to the antiglioma effect of the compound. Collectively, the $(PhSe)_2$-loaded polymeric nanocapsules arise as a promising candidate to future studies aiming at developing improved treatment to glioma.

Acknowledgements

We gratefully acknowledge UFSM, Fundo de Amparo à Pesquisa no Rio Grande do Sul (FAPERGS – 17/2551-0001041-8) and Coordenação de Aperfeiçoamento de Pessoal de nível Superior (CAPES-BR) for the financial support. L. M. Ferreira was granted a CAPES doctoral fellowship (1530525).

References

[1] Q.T. Ostrom, L. Bauchet, F.G. Davis, I. Deltour, J.L. Fisher, C.E. Langer, M. Pekmezci, J.A. Schwartzbaum, M.C. Turner, K.M. Walsh, M.R. Wrensch, J.S. Barnholtz-Sloan, The epidemiology of glioma in adults: a "state of the science" review, NeuroOncology 16 (7) (2014) 896–913.

[2] A. Behin, K. Hoang-Xuan, A.F. Carpentier, J.Y. Delattre, Primary brain tumours in adults, Lancet 361 (9354) (2003) 323–331.
[3] O.O. Kanu, A. Mehta, C.H. Di, N.J. Lin, K. Bortoff, D.D. Bigner, H. Yan, D.C. Adamson, Glioblastoma multiforme: a review of therapeutic targets, Expert Opin Ther Tar 13 (6) (2009) 701–718.
[4] R. Karim, C. Palazzo, B. Evrard, G. Piel, Nanocarriers for the treatment of glioblastoma multiforme: current state-of-the-art, J. Control. Release 227 (2016) 23–37.
[5] C.W. Nogueira, J.B.T. Rocha, Toxicology and pharmacology of selenium: emphasis on synthetic organoselenium compounds, Arch. Toxicol. 85 (11) (2011) 1313–1359.
[6] T. Posser, M.T. de Paula, J.L. Franco, R.B. Leal, J.B.T. da Rocha, Diphenyl diselenide induces apoptotic cell death and modulates ERK1/2 phosphorylation in human neuroblastoma SH-SY5Y cells, Arch. Toxicol. 85 (6) (2011) 645–651.
[7] F. Nedel, V.F. Campos, D. Alves, A.J.A. McBride, O.A. Dellagostin, T. Collares, L. Savegnago, F.K. Seixas, Substituted diaryl diselenides: cytotoxic and apoptotic effect in human colon adenocarcinoma cells, Life Sci. 91 (9-10) (2012) 345–352.
[8] L.M. Ferreira, V.F. Cervi, M.H.M. Sari, A.V. Barbieri, A.P. Ramos, P.M. Copetti, G.F. de Brum, R. Nascimento, J.M. Nadal, P.V. Farago, M.R. Sagrillo, C.W. Nogueira, L. Cruz, Diphenyl diselenide loaded poly(epsilon-caprolactone) nanocapsules with selective antimelanoma activity: development and cytotoxic evaluation, Mat Sci Eng C-Mater 91 (2018) 1–9.
[9] N.B.D. Barbosa, C.W. Nogueira, T.N. Guecheva, M.D. Bellinaso, J.B.T. Rocha, Diphenyl diselenide supplementation delays the development of N-nitroso-N-methylurea-induced mammary tumors, Arch. Toxicol. 82 (9) (2008) 655–663.
[10] M. Diaz, R. Gonzalez, D. Plano, J.A. Palop, C. Sanmartin, I. Encio, A diphenyldiselenide derivative induces autophagy via JNK in HTB-54 lung cancer cells, J. Cell. Mol. Med. 22 (1) (2018) 289–301.
[11] M.T. Melo, I.M. de Oliveira, I. Grivicich, T.N. Guecheva, J. Saffi, J.A.P. Henriques, R.M. Rosa, Diphenyl diselenide protects cultured MCF-7 cells against tamoxifen-induced oxidative DNA damage, Biomed. Pharmacother. 67 (4) (2013) 329–335.
[12] N.B.V. Barbosa, J.B.T. Rocha, G. Zeni, T. Emanuelli, M.C. Beque, A.L. Braga, Effect of organic forms of selenium on delta-aminolevulinate dehydratase from liver, kidney, and brain of adult rats, Toxicol Appl Pharm 149 (2) (1998) 243–253.
[13] R.M. Rosa, R. Roesler, A.L. Braga, J. Saffi, J.A.P. Henriques, Pharmacology and toxicology of diphenyl diselenide in several biological models, Braz. J. Med. Biol. Res. 40 (10) (2007) 1287–1304.
[14] M. Prigol, C.W. Nogueira, G. Zeni, M.R. Bronze, L. Constantino, Physicochemical and biochemical profiling of diphenyl diselenide, Appl. Biochem. Biotechnol. 169 (3) (2013) 885–893.
[15] M. Prigol, C.A. Bruning, F. Martini, C.W. Nogueira, Comparative excretion and tissue distribution of selenium in mice and rats following treatment with diphenyl diselenide, Biol. Trace Elem. Res. 150 (1-3) (2012) 272–277.
[16] C.F.A. Giordani, D. de Souza, L. Dornelles, C.W. Nogueira, M.P. Alves, M. Prigol, O.E.D. Rodrigues, Diphenyl diselenide-loaded nanocapsules: preparation and biological distribution, Appl. Biochem. Biotech. 172 (2) (2014) 755–766.
[17] S.T. Stefanello, F. Dobrachinski, N.R. de Carvalho, G.P. Amaral, R.P. Barcelos, V.A. Oliveira, C.S. Oliveira, C.F.A. Giordani, M.E. Pereira, O.E.D. Rodrigues, F.A.A. Soares, Free radical scavenging in vitro and biological activity of diphenyl diselenide-loaded nanocapsules: DPDS-NCS antioxidant and toxicological effects, Int. J. Nanomed. Nanosurg. 10 (2015).
[18] M.C.L. Marchiori, C. Rigon, P.M. Copetti, M.R. Sagrillo, L. Cruz, Nanoencapsulation improves scavenging capacity and decreases cytotoxicity of Silibinin and pomegranate oil association, AAPS PharmSciTech 18 (8) (2017) 3236–3246.
[19] M. Gehrcke, L.M. Giuliani, L.M. Ferreira, A.V. Barbieri, M.H.M. Sari, E.F. da Silveira, J.H. Azambuja, C.W. Nogueira, E. Braganhol, L. Cruz, Enhanced photostability, radical scavenging and antitumor activity of indole-3-carbinol-loaded rose hip oil nanocapsules, Mat. Sci. Eng. C-Mater. 74 (2017) 279–286.
[20] L.M. Ferreira, V.F. Cervi, M. Gehrcke, E.F. da Silveira, J.H. Azambuja, E. Braganhol, M.H.M. Sari, V.A. Zborowski, C.W. Nogueira, L. Cruz, Ketoprofen-loaded pomegranate seed oil nanoemulsion stabilized by pullulan: selective antiglioma formulation for intravenous administration, Colloids Surf. B Biointerfaces 130 (2015) 272–277.
[21] M.H.M. Sari, L.M. Ferreira, V. AngonesiZborowski, P.C.O. Araujo, J.M. Nadal, P.V. Farago, L. Cruz, C.W. Nogueira, p,p' -Methoxyl-diphenyl diselenideincorporation into polymeric nanocapsules improves its antinociceptive action: Physicochemical and behavioral studies, Colloids Surf. B Biointerfaces 157 (2017) 464–472.
[22] M.H.M. Sari, V.A. Zborowski, L.M. Ferreira, N.D. Jardim, P.C.O. Araujo, C.A. Bruning, L. Cruz, C.W. Nogueira, Enhanced pharmacological actions of p,p' -methoxyl-diphenyl diselenide-loaded polymeric nanocapsules in a mouse model of neuropathic pain: behavioral and molecular insights, J. Trace Elem. Med. Biol. 46 (2018) 17–25.
[23] M. Gehrcke, M.H.M. Sari, L.M. Ferreira, A.V. Barbieri, L.M. Giuliani, V.C. Prado, J.M. Nadal, P.V. Farago, C.W. Nogueira, L. Cruz, Nanocapsules improve indole-3-carbinol photostability and prolong its antinociceptive action in acute pain animal models, Eur. J. Pharm. Sci. 111 (2018) 133–141.
[24] L.A. Frank, R.V. Contri, R.C.R. Beck, A.R. Pohlmann, S.S. Guterres, Improving drug biological effects by encapsulation into polymeric nanocapsules, Wires Nanomed Nanobi 7 (5) (2015) 623–639.
[25] D.R. Nogueira, L.E. Scheeren, L.B. Macedo, A.I.P. Marcolino, M.P. Vinardell, M. Mitjans, M.R. Infante, A.A. Farooqi, C.M.B. Rolim, Inclusion of a pH-responsive amino acid-based amphiphile in methotrexate-loaded chitosan nanoparticles as a delivery strategy in cancer therapy, Amino Acids 48 (1) (2016) 157–168.
[26] E.F. da Silveira, J.M. Chassot, F.C. Teixeira, J.H. Azambuja, G. Debom, F.T. Beira, F.A.B. Del Pino, A. Lourenco, A.P. Horn, L. Cruz, R.M. Spanevello, E. Braganhol, Ketoprofen-loaded polymeric nanocapsules selectively inhibit cancer cell growth in vitro and in preclinical model of glioblastoma multiforme, Invest New Drug 31 (6) (2013) 1424–1435.
[27] G. Lollo, M. Vincent, G. Ullio-Gamboa, L. Lemaire, F. Franconi, D. Couez, J.P. Benoit, Development of multifunctional lipid nanocapsules for the co-delivery of paclitaxel and CpG-ODN in the treatment of glioblastoma, Int. J. Pharmaceut. 495 (2) (2015) 972–980.
[28] L.M. Ferreira, L.V.C. da Rosa, T.E. Müller, C.C. de Menezes, M.H. Marcondes Sari, V.L. Loro, C.W. Nogueira, D.B. Rosemberg, L. Cruz, Zebrafish exposure to diphenyl diselenide-loaded polymeric nanocapsules caused no behavioral impairments and brain oxidative stress, J. Trace Elem. Med. Biol. 53 (2019) 62–68.
[29] C. Paulmier, Selenoorganic functional groups. Selenium reagents and intermediates in organic synthesis, Angew. Chem 100 (1986) 25–51.
[30] D.J. Stuehr, C.F. Nathan, Nitric-oxide - a macrophage product responsible for cytostasis and respiratory inhibition in tumor target-cells, J. Exp. Med. 169 (5) (1989) 1543–1555.
[31] M.M. Bradford, A rapid and sensitive method for the quantitation of microgram quantities of protein utilizing the principle of protein-dye binding, Anal. Biochem. 72 (1-2) (1976) 248–254.
[32] G.L. Ellman, Tissue sulfhydryl groups, Arch. Biochem. Biophys. 82 (1) (1959) 70–77.
[33] A.Z. Reznick, L. Packer, Oxidative damage to proteins - spectrophotometric method for carbonyl assay, Method Enzymol 233 (1994) 357–363.
[34] S. Sassa, Delta-aminolevulinic-Acid dehydratase assay, Enzyme 28 (2-3) (1982) 133–143.
[35] H.P. Misra, I. Fridovich, The role of superoxide anion in the autoxidation of epinephrine and a simple assay for superoxide dismutase, J. Biol. Chem. 247 (1972) 3170–3175.
[36] W.H. Habig, M.J. Pabst, W.B. Jakoby, Glutathione S-Transferases - first enzymatic step in mercapturic acid formation, J. Biol. Chem. 249 (22) (1974) 7130–7139.
[37] H. Aebi, Catalase in vitro, Meth. Enzymol. 105 (1984) 121–126.
[38] O. Myhre, J.M. Andersen, H. Aarnes, F. Fonnum, Evaluation of the probes 2′,7′-dichlorofluorescin diacetate, luminol, and lucigenin as indicators of reactive species formation, Biochem. Pharmacol. 65 (10) (2003) 1575–1582.
[39] D.N. Louis, A. Perry, G. Reifenberger, A. von Deimling, D. Figarella-Branger, W.K. Cavenee, H. Ohgaki, O.D. Wiestler, P. Kleihues, D.W. Ellison, The 2016 World Health Organization Classification of Tumors of the Central Nervous System: a summary, Acta Neuropathol. 131 (6) (2016) 803–820.
[40] E.R. Laws, I.F. Parney, W. Huang, F. Anderson, A.M. Morris, A. Asher, K.O. Lillehei, M. Bernstein, H. Brem, A. Sloan, M.S. Berger, S. Chang, G.O. Investigators, Survival following surgery and prognostic factors for recently diagnosed malignant glioma: data from the Glioma Outcomes Project, J. Neurosurg. 99 (3) (2003) 467–473.
[41] I. Brigger, C. Dubernet, P. Couvreur, Nanoparticles in cancer therapy and diagnosis, Adv Drug Deliver Rev 54 (5) (2002) 631–651.
[42] F. Pourgholi, M. Hajivalili, J.N. Farhad, H.S. Kafil, M. Yousefi, Nanoparticles: novel vehicles in treatment of Glioblastoma, Biomed. Pharmacother. 77 (2016) 98–107.
[43] G. Caruso, M. Caffo, C. Alafaci, G. Raudino, D. Cafarella, S. Lucerna, F.M. Salpietro, F. Tomasello, Could nanoparticle systems have a role in the treatment of cerebral gliomas? NanomedNanotechnol 7 (6) (2011) 744–752.
[44] N.S. Pegoraro, J. Mattiazzi, E.F. da Silveira, J.H. Azambuja, E. Braganhol, L. Cruz, Improved photostability and cytotoxic effect of coenzyme Q10 by its association with vitamin E acetate in polymeric nanocapsules, Pharm. Dev. Technol. 23 (4) (2018) 400–406.
[45] A. Bernardi, E. Braganhol, E. Jager, F. Figueiro, M.I. Edelweiss, A.R. Pohlmann, S.S. Guterres, A.M. Battastini, Indomethacin-loaded nanocapsules treatment reduces in vivo glioblastoma growth in a rat glioma model, Cancer Lett. 281 (1) (2009) 53–63.
[46] D. Fukumura, S. Kashiwagi, R.K. Jain, The role of nitric oxide in tumour progression, Nat. Rev. Cancer 6 (7) (2006) 521–534.
[47] M. Lechner, P. Lirk, J. Rieder, Inducible nitric oxide synthase (iNOS) in tumor biology: the two sides of the same coin, Semin. Cancer Biol. 15 (4) (2005) 277–289.
[48] D. Lam-Himlin, M.G. Espey, G. Perry, M.A. Smith, R.J. Castellani, Malignant glioma progression and nitric oxide, Neurochem. Int. 49 (8) (2006) 764–768.
[49] C.C. Drewes, L.A. Fiel, C.G. Bexiga, A.C.C. Asbahr, M.K. Uchiyama, B. Cogliati, K. Araki, S.S. Guterres, A.R. Pohlmann, S.P. Farsky, Novel therapeutic mechanisms determine the effectiveness of lipid-core nanocapsules on melanoma models, Int. J. Nanomed. Nanosurg. 11 (2016) 1261–1279.
[50] D. Plesca, S. Mazumder, A. Almasan, DNA damage response and apoptosis, programmed cell death, the biology and therapeutic implications of cell death, Part B 446 (2008) 107–122.
[51] G. Lollo, G. Ullio-Gamboa, E. Fuentes, K. Matha, N. Lautram, J.P. Benoit, In vitro anti-cancer activity and pharmacokinetic evaluation of curcumin-loaded lipid nanocapsules, Mat Sci Eng C-Mater 91 (2018) 859–867.
[52] A. Bernardi, R.L. Frozza, E. Jager, F. Figueiro, L. Bavaresco, C. Salbego, A.R. Pohlmann, S.S. Guterres, A.M.O. Battastini, Selective cytotoxicity of indomethacin and indomethacin ethyl ester-loaded nanocapsules against glioma cell lines: an in vitro study, Eur. J. Pharmacol. 586 (1-3) (2008) 24–34.
[53] S. Aula, S. Lakkireddy, K. Jamil, A. Kapley, A.V.N. Swamyd, H.R. Lakkireddy, Biophysical, biopharmaceutical and toxicological significance of biomedical nanoparticles, RSC Adv. 5 (2015) 47830–47859.
[54] M. Prigol, R.F. Schumacher, C. WayneNogueira, G. Zeni, Convulsant effect of diphenyl diselenide in rats and mice and its relationship to plasma levels, Toxicol. Lett. 189 (1) (2009) 35–39.
[55] M.H.M. Sari, L.M. Ferreira, V.A. Zborowski, P.C.O. Araujo, V.F. Cervi, C.A. Bruning, L. Cruz, C.W. Nogueira, p,p'-Methoxyl-diphenyl diselenide-loaded polymeric nanocapsules are chemically stable and do not induce toxicity in mice, Eur. J. Pharm. Biopharm. 117 (2017) 39–48.
[56] X.B. Wang, Y.L. Jia, P. Wang, Q.H. Liu, H.R. Zheng, Current status and future perspectives of sonodynamic therapy in glioma treatment, Ultrason. Sonochem. 37 (2017) 592–599.
[57] F.B. Morrone, D.L. Oliveira, P. Gamermann, J. Stella, S. Wofchuk, M.R. Wink, L. Meurer, M.I.A. Edelweiss, G. Lenz, A.M.O. Battastini, In vivo glioblastoma growth is reduced by apyrase activity in a rat glioma model, BMC Cancer 6 (2006).